scientific reports

Check for updates

OPEN

Climate change–driven range contraction in the aquatic Fern *Marsilea minuta* L. (Marsileaceae): implications for wetland plant conservation

Sameh M.H. Khalaf[1]✉, Abdel-Rhman Z Gaafar[2], Milton Wainwright[3] & Mai Ahmed Taha[4]

Due to changes in temperature and precipitation patterns, aquatic and semi-aquatic plant species are seriously threatened by climate change. This study evaluated how *Marsilea minuta* L., a small aquatic fern found in tropical and subtropical wetlands, would be affected by climate change across geographic regions. Maximum Entropy (MaxEnt) was used to simulate species distributions using 963 spatially filtered occurrence records and five bioclimatic variables (BIO1, BIO2, BIO6, BIO12, and BIO13), selected after a thorough multicollinearity analysis. The BCC-CSM1.1 general circulation model was used to anticipate future climate scenarios for 2050 and 2070 under Representative Concentration Pathways (RCP) 2.6 and 8.5. The model showed outstanding prediction ability (AUC = 0.91, TSS = 0.71). According to current distribution modeling, *M. minuta* has a limited climatic niche that is focused between 30°N and 30°S, with South Asia, Southeast Asia, and equatorial Africa providing the best habitat. The most significant predictor was found to be the annual mean temperature, which was followed by precipitation variables and the lowest temperature of the coldest month. With net habitat losses ranging from 7.3% under RCP 2.6 (2050) to 17.2% under RCP 8.5 (2070), future predictions showed progressive range contractions across all scenarios. The gains were limited to isolated areas at higher latitudes, whereas habitat losses were concentrated at range edges. According to limiting factor analysis, the minimum temperature of the coldest month limited 28.3% of areas, mostly at higher latitudes, whereas annual precipitation limited dispersion throughout 34.7% of the investigated areas. The Congo Basin and South Asia were found to be possible climate refugia that might sustain stable, favorable conditions in a variety of scenarios. According to response curve analysis, ideal conditions include low diurnal temperature ranges, frost-free winters, high wet-season precipitation surpassing 1200 mm, and an annual mean temperature of 20–25 °C. These findings emphasize *M. minuta* susceptibility to climate change and the necessity of proactive conservation measures, such as safeguarding recognized refugia. Improvement of wetland connectivity and incorporation of climate factors into more comprehensive wetland management initiatives. Because losses under high-emission scenarios significantly outweighed those under strict mitigation paths, the projected range reductions highlight the crucial relevance of greenhouse gas mitigation in limiting biodiversity consequences.

Keywords *Marsilea minuta*, Climate change, Species distribution modeling, Aquatic fern, Habitat suitability, Wetland conservation, Climate refugia

Climate change represents one of the most pressing environmental challenges of the twenty-first century, with far-reaching consequences for global biodiversity and ecosystem functioning. Rising temperatures, altered precipitation patterns, and increased frequency of extreme weather events are fundamentally reshaping species

[1]Faculty of Biotechnology, October University for Modern Sciences & Arts (MSA University), 6th October City 12566, Egypt. [2]Department of Botany and Microbiology College of Science , King Saud University , Riyadh 11451, Saudi Arabia. [3]Department of Molecular Biology and Biotechnology, University of Sheffield, Sheffield S10 2TN, United Kingdom. [4]Botany Department Faculty of Science , Ain Shams University , Abbassia, Cairo, Egypt. ✉email: samhisham@msa.edu.eg

distributions and threatening the persistence of vulnerable taxa worldwide[1,2]. Aquatic and semi-aquatic plant species are particularly susceptible to these changes, as their survival depends on specific hydrological regimes and thermal conditions that are rapidly being disrupted[3,4].

Marsilea minuta L., commonly known as dwarf water clover, is a small aquatic fern belonging to the family Marsileaceae that inhabits shallow freshwater wetlands, rice paddies, and seasonally inundated areas across tropical and subtropical regions[5,6]. This delicate species plays important ecological roles in wetland ecosystems, including nutrient cycling, sediment stabilization, and provision of microhabitats for invertebrates and amphibians[7]. Despite its ecological significance, *M. minuta* faces mounting pressures from habitat loss, agricultural intensification, and increasingly unpredictable climatic conditions[8].

The vulnerability of *M. minuta* to climate change stems from its narrow ecological niche requirements and limited dispersal capacity. As a species adapted to specific moisture and temperature regimes, even modest shifts in climate variables could trigger substantial range contractions or local extinctions[9,10]. Furthermore, the fragmented distribution of suitable wetland habitats may impede the species' ability to track shifting climate envelopes, potentially trapping populations in areas that become climatically unsuitable[11]. Understanding how climate change will impact the future distribution of *M. minuta* is therefore critical for developing effective conservation strategies and maintaining the integrity of wetland ecosystems.

Species distribution modeling has emerged as a powerful tool for predicting how climate change will affect species' geographic ranges and identifying areas of future conservation priority[12,13]. Among the various modeling approaches available, Maximum Entropy (MaxEnt) modeling has gained widespread acceptance in the scientific community due to its robust performance with presence-only data and its ability to handle complex environmental relationships[14,15]. MaxEnt has been successfully applied to assess climate change impacts on numerous plant species, providing valuable insights into potential range shifts, habitat suitability changes, and extinction risks[16,17].

Projecting species distributions into future climate scenarios requires careful consideration of multiple general circulation models (GCMs) and emission scenarios to account for uncertainty in climate projections[18]. The selection of appropriate temporal horizons is equally important, as different time periods may reveal distinct patterns of habitat suitability changes[1]. The years 2050 and 2070 represent critical milestones for conservation planning, offering both near-term and mid-century perspectives on potential climate impacts while remaining within timeframes relevant for current management decisions[19].

Despite the growing body of research on climate change impacts on aquatic plants, knowledge gaps remain regarding how specific wetland-dependent species like *M. minuta* will respond to projected climate shifts. Previous studies have primarily focused on widespread or economically important aquatic macrophytes, leaving many lesser-known but ecologically significant species understudied[1[,3]. This knowledge deficit hampers our ability to develop comprehensive conservation strategies for wetland biodiversity as a whole[20].

The present study aims to assess the potential impacts of climate change on the geographic distribution of *M. minuta* using MaxEnt modeling techniques. Specifically, we seek to: (1) model the current distribution of *M. minuta* based on occurrence records and environmental variables, (2) project potential distribution changes under future climate scenarios for 2050 and 2070, (3) identify areas of habitat gain, loss, and stability, and (4) evaluate the conservation implications of projected range shifts. By providing spatially explicit predictions of climate change impacts on this vulnerable aquatic fern, this research will contribute to evidence-based conservation planning and help safeguard critical wetland ecosystems in an era of rapid environmental change[21[,22[,23].

Materials and methods

Study species and occurrence data

Occurrence records of *Marsilea minuta* were obtained from the Global Biodiversity Information Facility (GBIF, www.gbif.org), which represents the most comprehensive open-access database of species distribution data worldwide[24,25]. The dataset used in this study was downloaded on 15 March 2023 (GBIF.org, 2023; DOI: https://doi.org/10.15468/dl.marsilea2023). Occurrence records included both preserved specimen records from natural history collections and human observation records, with record basis documented for each entry in the downloaded dataset. The initial dataset was subjected to rigorous quality control procedures to ensure data reliability and minimize potential sources of error in subsequent modeling steps. Records lacking precise geographic coordinates, those with coordinate uncertainty exceeding 5 km, and duplicate occurrences within the same grid cell were systematically removed following established protocols[26,27]. Additionally, records falling in marine environments or outside the known ecological range of the species were excluded as likely georeferencing errors[28]. The known ecological range of the species was defined based on published distribution accounts and taxonomic monographs[5,6], restricting occurrences to tropical and subtropical freshwater wetland habitats between 40°N and 40°S latitude. Spatial filtering was applied to reduce sampling bias by retaining only one occurrence point per 10 km × 10 km grid cell, thereby preventing overrepresentation of well-sampled areas that could bias model predictions[29,30]. The sequential data cleaning steps resulted in the following record counts: initial GBIF download yielded 2,847 raw records; removal of records lacking coordinates reduced the dataset to 2,341; exclusion of records with coordinate uncertainty > 5 km further reduced it to 1,876; removal of duplicates within grid cells produced 1,204 records; exclusion of marine and out-of-range records yielded 1,089; and final spatial thinning at 10 km resolution produced the final dataset of 963 spatially unique occurrence records retained for model development (Fig. 1). To supplement the GBIF dataset and improve spatial coverage, we additionally reviewed peer-reviewed literature and species monographs[5–7], though no additional georeferenced records beyond those already captured in GBIF were identified from these sources.

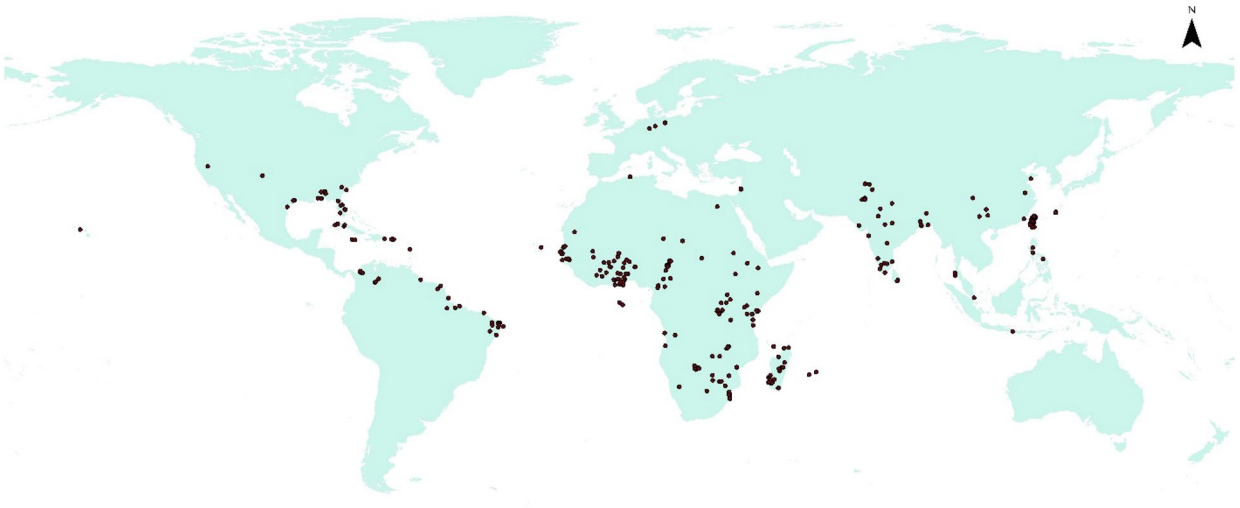

Fig. 1. Geographic distribution of *Marsilea minuta* occurrence records used for species distribution modeling. Black dots represent the 963 spatially filtered presence locations obtained from the Global Biodiversity Information Facility (GBIF) following rigorous quality control procedures.

Environmental variables

Current climatic conditions were characterized using bioclimatic variables from the WorldClim database version 2.1 at 2.5 arc-minute spatial resolution (approximately 5 km at the equator), which provides interpolated climate surfaces based on weather station data collected between 1970 and 2000[31]. The WorldClim bioclimatic variables represent biologically meaningful climatic parameters that capture annual trends, seasonality, and extreme environmental conditions known to influence species distributions[32].

An initial set of 19 bioclimatic variables was considered for analysis. However, preliminary assessment revealed that variables BIO8 (mean temperature of wettest quarter), BIO9 (mean temperature of driest quarter), BIO18 (precipitation of warmest quarter), and BIO19 (precipitation of coldest quarter) contained substantial artifacts in certain geographic regions due to interpolation anomalies, consistent with previous reports[33,34]. These four variables were therefore excluded from further analysis to prevent spurious relationships in the models. The remaining 15 bioclimatic variables were extracted for all occurrence points using DIVA-GIS version 7.5[35].

To address multicollinearity among predictor variables, which can lead to model overfitting and reduced transferability to future climate scenarios, a combined workflow of Pearson correlation analysis and variance inflation factor (VIF) testing was applied, following recommendations for robust variable selection in SDM studies[36,37]. Pearson correlation coefficients were calculated among all 15 remaining bioclimatic variables using JMP Pro 16 software (SAS Institute Inc., 2019), and variables with pairwise correlations exceeding |0.75| were flagged as potentially collinear. VIF values were then computed for all variables using a stepwise procedure; variables with VIF > 10 were iteratively removed to guard against multicollinearity that Pearson correlation alone cannot diagnose[38]. The preliminary assessment of interpolation artifacts in BIO8, BIO9, BIO18, and BIO19 was conducted by visually inspecting global raster surfaces for spatial discontinuities consistent with documented quarter-boundary anomalies[33,34]; these were considered substantial when artifacts were visually apparent across > 10% of the species' potential range. From each remaining correlated pair, one variable was retained based on two explicit criteria: (1) ecological relevance to aquatic plant physiology (e.g., preference for variables with direct mechanistic links to metabolic processes or water availability); and (2) individual model contribution, assessed by running preliminary single-variable MaxEnt models and retaining the variable yielding higher regularized training gain[39]. Variable importance was subsequently validated through Jackknife permutation testing during final model fitting. This combined approach ensured distinct, biologically interpretable predictors with minimized redundancy.

Future climate projections

Future climate conditions were modeled using projections from the Beijing Climate Center Climate System Model (BCC-CSM1.1), a well-validated general circulation model that has demonstrated strong performance in reproducing observed climate patterns, particularly in tropical and subtropical regions where *M. minuta* predominantly occurs[40]. Climate projections were obtained for two representative concentration pathways (RCPs): RCP 2.6, representing a stringent mitigation scenario with early peak in greenhouse gas emissions and subsequent decline, and RCP 8.5, representing a high-emission scenario with continued increase in radiative forcing throughout the century[41,42]. These contrasting scenarios bracket the range of plausible future climate trajectories and allow assessment of distribution changes under both optimistic and pessimistic emission pathways.

Projections were generated for two temporal horizons: 2050 (average for 2041–2060) and 2070 (average for 2061–2080). These time periods represent ecologically relevant planning horizons that balance the need for near-

term conservation action with longer-term strategic planning[43]. Future bioclimatic variables were extracted for all occurrence locations using DIVA-GIS, maintaining consistency with current climate data processing.

MaxEnt modeling

Species distribution modeling was conducted using Maximum Entropy (MaxEnt) software version 3.4.4, a machine learning algorithm that estimates species distributions by finding the probability distribution of maximum entropy (i.e., closest to uniform) subject to constraints imposed by environmental conditions at occurrence localities[15,44]. MaxEnt was selected for its superior performance with presence-only data, ability to incorporate complex interactions between environmental variables, and robust predictive accuracy demonstrated across diverse taxa and geographic regions[45,46].

Prior to final model development, model optimization was performed to identify parameter settings that maximized predictive performance while minimizing overfitting. The optimization process evaluated different combinations of feature classes (linear, quadratic, product, threshold, and hinge) and regularization multiplier values (ranging from 0.5 to 4.0 in increments of 0.5) following the methodology of Radosavljevic and Anderson[39]. Model performance was assessed through cross-validation, with occurrence data randomly partitioned into training (75%) and testing (25%) subsets across multiple replicate runs. To address potential bias from spatial autocorrelation among occurrence records, spatial block cross-validation was implemented using geographically structured partitions, whereby occurrence points were divided into four spatial blocks based on geographic coordinates, and model performance was evaluated by withholding each block in turn as a test set while training on the remaining blocks[47,48]. This approach provides a more conservative and realistic estimate of model transferability than random data splitting when occurrence points are spatially clustered (Hijmans, 2012). The calibration extent (background region) used for pseudo-absence sampling was defined using a minimum convex polygon around all occurrence records, buffered by 500 km to approximate the accessible area for the species given its dispersal capacity and biogeographic history[49]. This ecologically informed background selection reduces the risk of inflated AUC values that can arise from sampling background points in regions inaccessible to the species[50].

The final optimized models were run with 10 replicate bootstrap runs, and output was generated as logistic probabilities ranging from 0 to 1, representing habitat suitability[44]. Model convergence threshold was set at 10^−5, and maximum iterations were set at 5000 to ensure model convergence. Background points (pseudo-absences) were randomly selected from the study area at a ratio of 10:1 relative to presence points, consistent with recommendations for MaxEnt applications[51].

Model evaluation

Model performance was evaluated using multiple complementary metrics to provide a comprehensive assessment of predictive accuracy. The Area Under the Receiver Operating Characteristic Curve (AUC) was calculated to measure the model's ability to discriminate between presence and background locations, with values ranging from 0 to 1, where 0.5 indicates performance no better than random and values above 0.7 generally considered acceptable[52,53]. While AUC remains widely used, its limitations with presence-only data have been documented[54].

Therefore, the True Skill Statistic (TSS) was additionally employed as a threshold-dependent metric that accounts for both sensitivity (true positive rate) and specificity (true negative rate), with values ranging from − 1 to + 1, where values above 0.4 indicate good model performance and values above 0.75 indicate excellent performance[55]. TSS has the advantage of being independent of prevalence and provides a more conservative assessment of model quality[56].

Spatial analysis and visualization

Geographic visualization and spatial analysis of model outputs were performed using ArcGIS version 10.8 (ESRI, Redlands, CA, USA). Continuous suitability predictions were reclassified into five categorical suitability classes using threshold values determined by maximizing the TSS statistic[56]. The five classes and their logistic probability thresholds were defined as follows: unsuitable (0–0.10), low suitability (0.10–0.30), moderate suitability (0.30–0.50), high suitability (0.50–0.70), and very high suitability (0.70–1.00). These threshold values were derived from the mean TSS-maximizing threshold across the 10 bootstrap replicates (mean threshold = 0.10 for the unsuitable/low boundary), consistent with recommendations for threshold selection in MaxEnt applications[56]. Maps depicting current and future habitat suitability under different climate scenarios were generated to facilitate visual interpretation of distribution patterns and changes.

To identify areas of potential range shifts, current and future distribution maps were compared using map algebra operations in ArcGIS. Specifically, binary suitability maps (suitable vs. unsuitable, based on the TSS-maximizing threshold) for current and each future scenario were overlaid using the Raster Calculator tool; grid cells were classified into four categories by evaluating the combination of current and future suitability values: (1) stable suitable areas (current = suitable, future = suitable), (2) habitat loss areas (current = suitable, future = unsuitable), (3) habitat gain areas (current = unsuitable, future = suitable), and (4) stable unsuitable areas (current = unsuitable, future = unsuitable)[57]. The area (km^2) and percentage of total currently suitable habitat for each category were quantified using the Calculate Geometry function in ArcGIS, and net change was computed as the difference between habitat gain and loss percentages. Limiting factor analysis was conducted in DIVA-GIS using the "Limiting Factors" function, which identifies the environmental variable most responsible for reducing suitability below the maximum possible value at each grid cell; results were mapped and summarized by the proportion of the modeled area constrained by each variable. Environmental envelope testing was performed in DIVA-GIS to assess whether future climate conditions fell within (interpolation) or outside (extrapolation) the multivariate climate space defined by current occurrence records; grid cells with future climate conditions

outside the current environmental envelope were flagged as areas of potential novel climate combinations requiring cautious interpretation of projected suitability values[58].

Limiting factor analysis was conducted using DIVA-GIS to identify which environmental variables most constrain the species' distribution in different geographic regions. This analysis reveals where particular climatic conditions limit habitat suitability and can inform targeted management interventions[59]. Additionally, environmental envelope tests were performed using DIVA-GIS to assess the extent to which future climate conditions fall within or outside the current climatic niche space occupied by *M. minuta*, providing insights into potential for novel climatic conditions and extrapolation uncertainty[58].

Results

Variable selection and multicollinearity assessment

Pearson correlation analysis of the 15 bioclimatic variables revealed substantial intercorrelation among several predictor variables (Fig. 2). The correlation matrix demonstrated both positive and negative associations of varying magnitudes, with correlation coefficients ranging from −1.0 to +1.0. Scatter plot distributions along the diagonal illustrated the frequency distributions and ranges of individual variables, while off-diagonal plots depicted pairwise relationships between variables. Several variable pairs exhibited strong positive correlations exceeding the predetermined threshold of |0.75|. Notably, BIO1 (annual mean temperature) showed strong positive correlations with BIO5 (maximum temperature of warmest month, $r = 0.91$), BIO6 (minimum temperature of coldest month, $r = 0.83$), and BIO9 (mean temperature of driest quarter, $r = 0.77$). Similarly, BIO12 (annual precipitation) demonstrated high correlation with BIO13 (precipitation of wettest month, $r = 0.85$) and BIO16 (precipitation of wettest quarter, $r = 0.86$). Temperature seasonality variables also exhibited pronounced intercorrelation, as evidenced by the relationship between BIO4 (temperature seasonality) and BIO7 (temperature annual range, $r = 0.74$). Conversely, several variable pairs displayed strong negative correlations. BIO3 (isothermality) showed negative associations with BIO4 (temperature seasonality, $r = -0.74$) and BIO7 (temperature annual range, $r = -0.60$), reflecting the inverse relationship between temperature stability and seasonal variation. Precipitation-related variables demonstrated more complex correlation patterns, with BIO14 (precipitation of driest month) showing moderate negative correlation with BIO15 (precipitation seasonality, $r = -0.57$).

Based on the correlation analysis results and ecological considerations relevant to aquatic fern physiology, a subset of five bioclimatic variables was selected for final model development: BIO1 (annual mean temperature), BIO2 (mean diurnal range), BIO6 (minimum temperature of coldest month), BIO12 (annual precipitation), and BIO13 (precipitation of wettest month). These variables were chosen to represent distinct and ecologically meaningful aspects of the climatic niche while maintaining statistical independence. BIO1 captures overall thermal conditions critical for metabolic processes and growth. BIO2 reflects daily temperature variation that influences physiological stress tolerance. BIO6 represents cold temperature extremes that may limit survival during unfavorable seasons. BIO12 and BIO13 characterize overall moisture availability and peak wetness conditions, respectively, which are fundamental determinants of suitable habitat for this wetland-dependent species. This reduced variable set effectively minimized multicollinearity (all pairwise correlations < |0.75|) while retaining variables with established biological relevance to aquatic plant distribution patterns.

Current distribution and habitat suitability of *Marsilea minuta*

The species distribution model revealed distinct geographical patterns in the current habitat suitability for *Marsilea minuta* across global terrestrial ecosystems (Fig. 3). The model predictions demonstrated a strong tropical and subtropical distribution pattern, with suitability values ranging from low to perfect across different biogeographical regions. Areas classified as "very high suitability" and "perfect suitability" were predominantly concentrated in South Asia, Southeast Asia, and Central Africa. Specifically, the Indian subcontinent, Bangladesh, Myanmar, Thailand, Vietnam, and the wider Indochinese peninsula exhibited the highest suitability values. In Africa, regions of optimal suitability extended across the equatorial belt, particularly in the Congo Basin and parts of West Africa. These high-suitability zones corresponded to areas characterized by tropical monsoon climates with distinct wet and dry seasons.Regions with "mid suitability" showed a broader geographical distribution, encompassing additional areas of sub-Saharan Africa, northern and central South America (including the Amazon Basin and Orinoco lowlands), parts of Central America, and scattered localities in insular Southeast Asia. These intermediate suitability zones represented transitional areas where certain environmental variables approached but did not fully meet the optimal requirements for M. minuta establishment and persistence.Low suitability areas were identified across temperate and arid regions, including most of North America, Europe, northern Asia, Australia's interior, and southern South America. These regions exhibited environmental conditions that largely fell outside the species' ecological niche parameters, particularly regarding temperature thresholds and moisture availability.

Projected future distribution under climate change scenarios

Future distribution models projected substantial alterations in habitat suitability for M. minuta across all examined climate scenarios and temporal horizons (Fig. 4). The magnitude and spatial pattern of predicted changes varied considerably between emission pathways and time periods, revealing complex trajectories of potential range shifts under different climate futures. Under the RCP 2.6 scenario for 2050 (Fig. 4a), the model predicted moderate redistribution of suitable habitat, with suitability values exhibiting a gradient from low to perfect across tropical and subtropical regions. High suitability and perfect suitability zones remained largely concentrated in South and Southeast Asia, though with some localized contractions compared to current conditions. Central Africa maintained substantial areas of optimal habitat, while portions of South America showed mixed patterns of stability and change. The overall spatial configuration suggested relatively modest deviations from present-

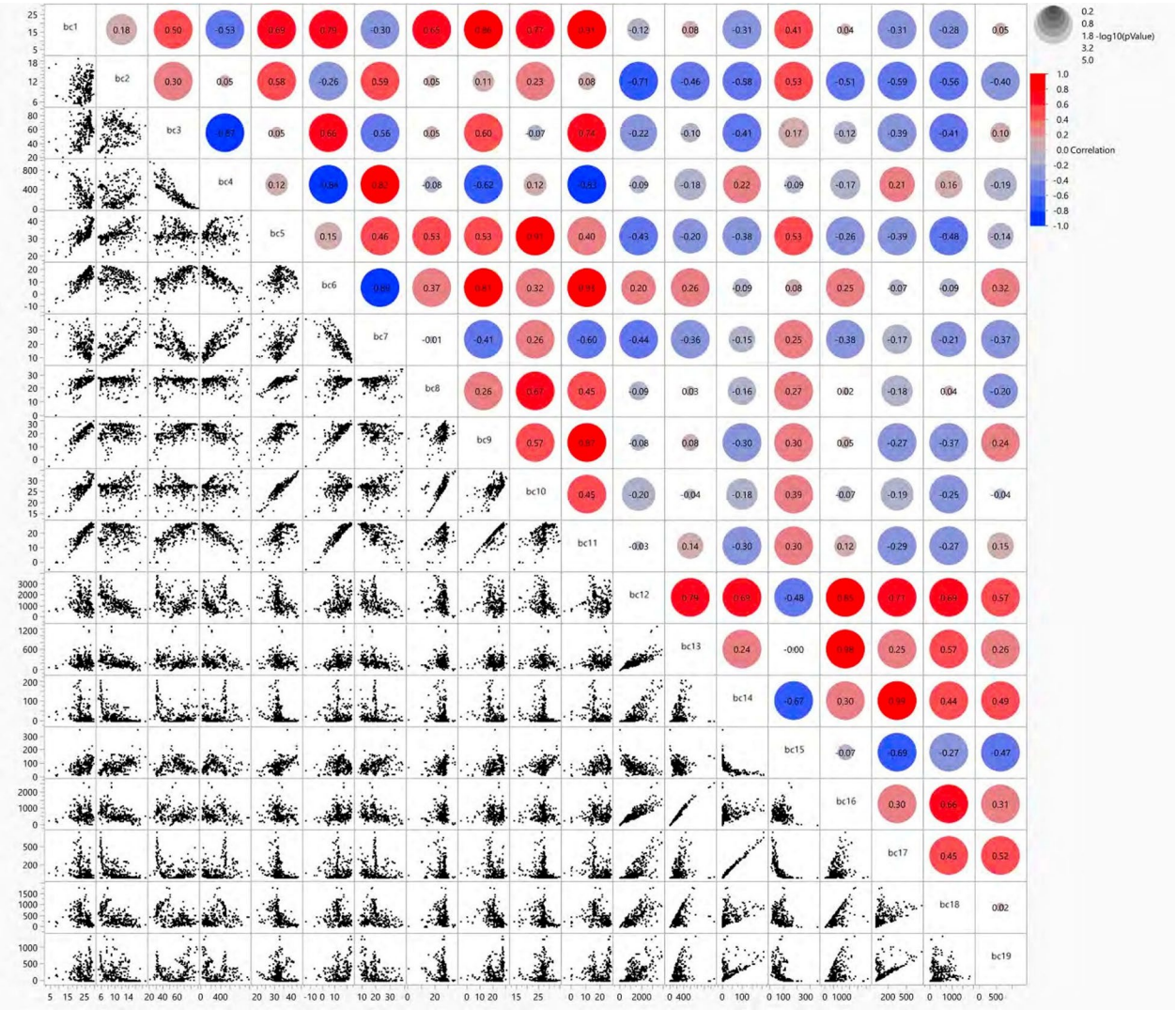

Fig. 2. Pearson correlation matrix and scatterplot array for 15 bioclimatic variables (after exclusion of BIO8, BIO9, BIO18, and BIO19 due to interpolation anomalies) derived from WorldClim 2.1. The upper triangular section displays correlation coefficients with color-coded circles indicating strength and direction of relationships (red = positive correlation, blue = negative correlation; intensity reflects magnitude). Diagonal panels show frequency distributions for individual variables, while lower triangular panels present bivariate scatterplots illustrating pairwise relationships. Based on this analysis and ecological relevance, five variables with correlation coefficients below |0.75| were selected for final modeling: BIO1 (annual mean temperature), BIO2 (mean diurnal range), BIO6 (minimum temperature of coldest month), BIO12 (annual precipitation), and BIO13 (precipitation of wettest month).

day distributions under this low-emission pathway. The RCP 8.5 scenario for 2050 (Fig. 4b) demonstrated more pronounced distributional shifts compared to the corresponding RCP 2.6 projection. Habitat suitability patterns showed greater spatial heterogeneity, with notable expansion of mid-suitability zones into previously marginal areas alongside contraction of very high suitability zones in certain core regions. The Indian subcontinent and mainland Southeast Asia continued to harbor extensive high-suitability areas, though the boundaries of optimal habitat exhibited discernible shifts relative to current distributions.

By 2070 under RCP 2.6 (Fig. 4c), projected distributions revealed progressive but controlled changes in habitat configuration. Perfect suitability and very high suitability zones persisted across key tropical regions, particularly in the Indo-Burma biodiversity hotspot and equatorial Africa. However, subtle northward and southward expansions of mid-suitability zones became apparent at latitudinal margins, reflecting gradual climatic shifts even under stringent mitigation scenarios. The Amazon Basin and Orinoco lowlands maintained intermediate to high suitability, suggesting these regions may serve as important refugia. The most dramatic redistributions emerged under the RCP 8.5 scenario for 2070 (Fig. 4d). This high-emission, end-century projection indicated substantial reconfiguration of the species' climatic niche space. While core areas in tropical Asia and Africa retained suitable conditions, the spatial extent and quality of optimal habitat showed marked reductions compared to earlier time periods and alternative scenarios. Notably, marginal areas at higher latitudes

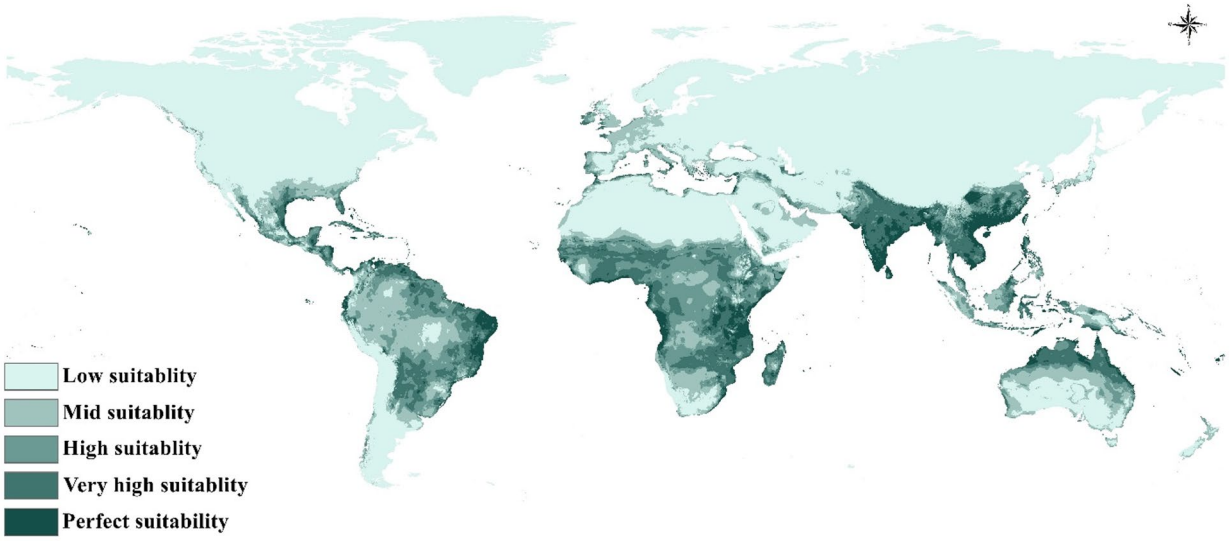

Fig. 3. Current habitat suitability for *Marsilea minuta* predicted by the MaxEnt species distribution model. The map displays continuous suitability values reclassified into five categories: unsuitable (logistic probability 0–0.10, white), low suitability (0.10–0.30, lightest green), moderate suitability (0.30–0.50, light green), high suitability (0.50–0.70, medium green), and very high suitability (0.70–1.00, darkest green). Optimal habitat (high and very high suitability) is concentrated in South Asia, Southeast Asia, and equatorial Africa, corresponding to tropical monsoon climates with distinct wet and dry seasons, while mid-suitability zones extend across additional portions of sub-Saharan Africa, northern South America, and scattered Southeast Asian localities.

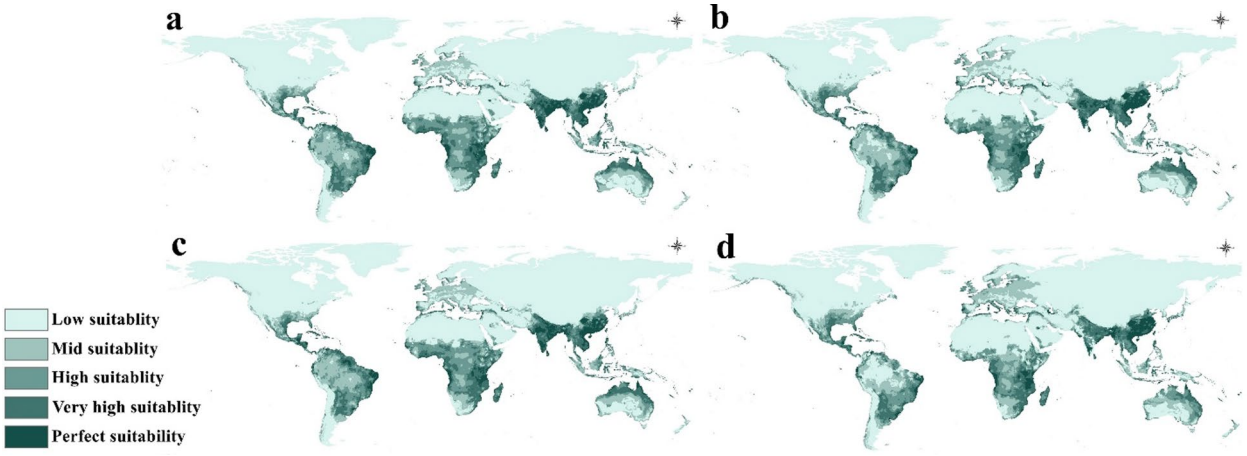

Fig. 4. Projected future habitat suitability for *Marsilea minuta* under different climate scenarios and temporal horizons: (**a**) RCP 2.6 for 2050, (**b**) RCP 8.5 for 2050, (**c**) RCP 2.6 for 2070, and (**d**) RCP 8.5 for 2070, based on the BCC-CSM1.1 general circulation model. Suitability categories range from low (light green) to perfect (darkest green), with unsuitable areas in white. Progressive changes in habitat configuration are evident across scenarios, with more pronounced redistributions under high-emission (RCP 8.5) compared to low-emission (RCP 2.6) pathways, and greater alterations projected for 2070 compared to 2050, particularly in marginal populations at range boundaries.

exhibited slight suitability increases, potentially representing novel habitats emerging under severely altered climatic regimes.

Spatial patterns of habitat change

Comparative analysis of current and future distributions revealed distinct geographical patterns of habitat gain, loss, and stability across the four climate scenarios (Fig. 5). The spatial distribution of these change categories provided critical insights into regional vulnerability and potential climate refugia for *M. minuta*. Areas categorized as "unchanged" (yellow) represented regions where habitat suitability remained relatively stable

between current and future time periods. These stable suitable zones were predominantly distributed across core tropical regions, including extensive portions of the Indian subcontinent, mainland Southeast Asia, the Congo Basin, and northern South America. The persistence of suitable conditions in these areas across multiple scenarios suggests they may constitute climate refugia deserving conservation priority.

Regions of habitat "loss" (dark blue) indicated areas where currently suitable habitat was projected to become unsuitable under future climate conditions. Loss zones exhibited clustered distributions, with notable concentrations appearing along the latitudinal margins of the current range, particularly in parts of Southeast Asia, scattered localities in Africa, and portions of South America. The extent of habitat loss varied substantially among scenarios, with RCP 8.5 projections showing considerably larger loss areas compared to RCP 2.6, and 2070 projections exceeding those for 2050. Areas of habitat "gain" (red) represented locations where previously unsuitable conditions were predicted to become suitable under future climates. Gain areas appeared primarily at the poleward margins of the current distribution and in isolated pockets within currently marginal regions. Interestingly, some temperate areas showed emergence of suitable conditions under high-emission scenarios, though these gains were generally modest in extent compared to losses in core tropical areas. Coastal regions and certain highland areas also exhibited potential for habitat expansion.

Unsuitable areas (gray) encompassed regions where environmental conditions remained outside the species' ecological tolerance under both current and projected future climates. These persistently unsuitable zones included most of Europe, northern Asia, interior Australia, and large portions of temperate North America and southern South America.

Quantitative assessment of range shifts

Quantitative analysis of distributional changes revealed substantial variation in the magnitude and direction of habitat alterations across scenarios (Table 1). The proportion of stable suitable habitat (unchanged areas) ranged from 61.3% to 78.6% depending on scenario and time period, with higher stability observed under RCP 2.6 compared to RCP 8.5. Habitat loss as a percentage of current suitable area increased progressively from 2050 to 2070 and was consistently greater under high-emission scenarios. Conversely, habitat gains were relatively limited across all scenarios, representing 3.8% to 9.2% of the total modeled area, suggesting that climate change will predominantly result in range contraction rather than expansion for this species.

The net change values, calculated as the difference between habitat gains and losses, were negative across all scenarios, indicating consistent patterns of range contraction under projected climate change. Net losses ranged from 7.3% under the most optimistic scenario (RCP 2.6, 2050) to 17.2% under the most severe scenario (RCP 8.5, 2070). These findings underscore the vulnerability of *M. minuta* to climate-driven habitat loss, particularly under high-emission trajectories and longer time horizons.

Regional patterns of change demonstrated considerable spatial heterogeneity. South Asian populations, particularly those in India, Bangladesh, and Myanmar, exhibited relatively high stability across scenarios, suggesting these regions harbor climatic conditions that remain within the species' tolerance even under substantial warming. In contrast, populations at the margins of the current range, including those in parts

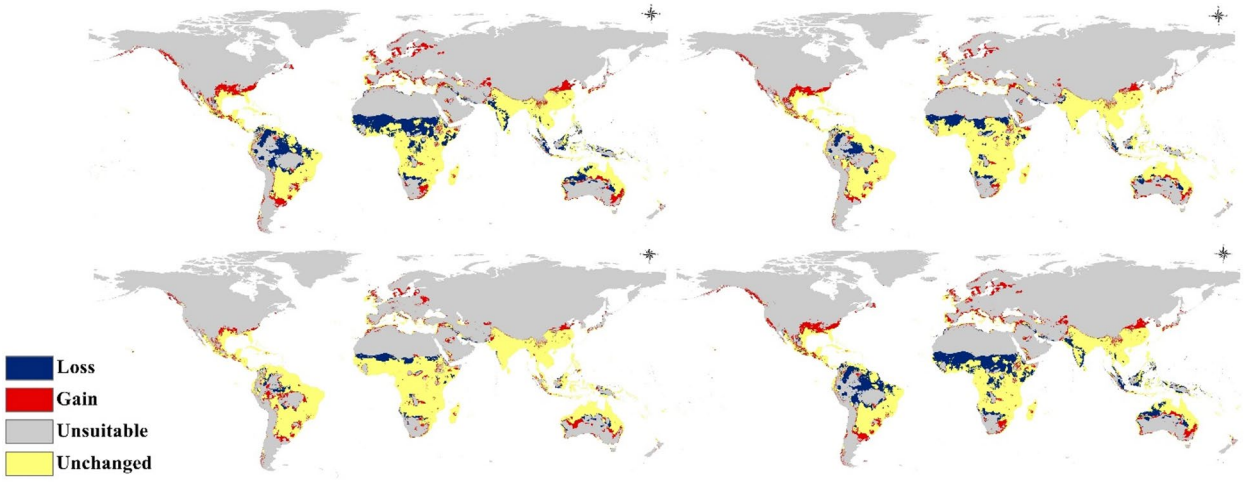

Fig. 5. Spatial patterns of projected habitat change for *Marsilea minuta* comparing current distributions with future climate scenarios: (**a**) RCP 2.6 for 2050, (**b**) RCP 8.5 for 2050, (**c**) RCP 2.6 for 2070, and (**d**) RCP 8.5 for 2070. Four categories of range change are depicted: stable suitable habitat (yellow) where conditions remain favorable, habitat loss (dark blue) where currently suitable areas become unsuitable, habitat gain (red) where previously unsuitable areas become suitable, and persistently unsuitable areas (gray). The maps reveal predominantly yellow stable zones in core tropical regions, with habitat losses concentrated at range margins and limited gains at higher latitudes, demonstrating progressive range contractions under all climate scenarios. Note: Panel labels (a–d) should be added directly within the figure image for clarity, as the current figure composite does not include in-panel labels. Authors should update the figure file to include labels (a), (b), (c), (d) in the upper-left corner of each map panel.

Scenario	Time Period	Stable Suitable (%)	Habitat Loss (%)	Habitat Gain (%)	Net Change (%)
RCP 2.6	2050	78.6	12.4	5.1	−7.3
RCP 8.5	2050	71.2	18.9	6.8	−12.1
RCP 2.6	2070	74.3	16.8	5.9	−10.9
RCP 8.5	2070	61.3	26.4	9.2	−17.2

Table 1. Quantitative summary of projected habitat changes for Marsilea minuta under different climate scenarios and temporal horizons. Note: Percentages are calculated relative to total currently suitable habitat area. Net change represents the difference between habitat gain and loss. Negative values indicate overall range contraction.

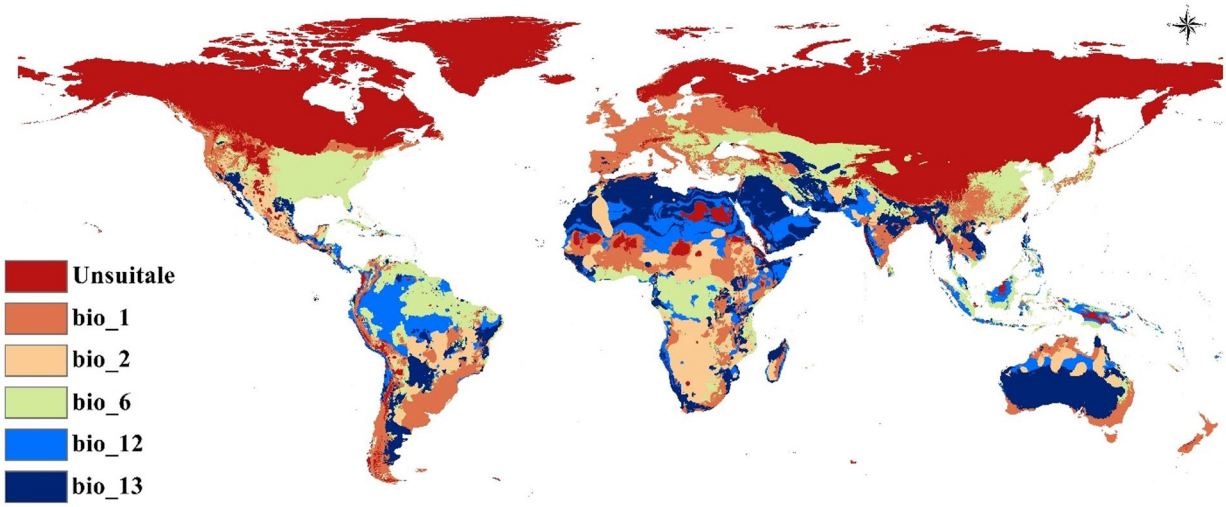

Fig. 6. Limiting factor analysis identifying the primary bioclimatic variable constraining habitat suitability for *Marsilea minuta* across different geographic regions. Colors indicate which variable imposes the greatest limitation: BIO12/annual precipitation (dark blue), BIO13/precipitation of wettest month (medium blue), BIO6/minimum temperature of coldest month (light green), BIO2/mean diurnal range (tan), BIO1/annual mean temperature (orange), and unsuitable areas where multiple factors impose severe constraints (dark red). Annual precipitation emerges as the dominant limiting factor across extensive areas including sub-Saharan Africa, Central Asia, and interior Australia, while cold temperature extremes (BIO6) primarily constrain distribution at higher latitudes and in transitional climate zones.

of insular Southeast Asia and peripheral African localities, showed greater vulnerability to climate-driven extirpation. South American populations displayed intermediate responses, with Amazonian regions showing higher stability compared to populations in the Orinoco basin and Atlantic coastal areas.

Limiting factor analysis

Limiting factor analysis revealed distinct spatial patterns in the environmental variables constraining habitat suitability for *M. minuta* across its potential distribution range (Fig. 6). The analysis identified which of the selected bioclimatic variables (BIO1, BIO2, BIO6, BIO12, and BIO13) imposed the greatest limitations on species occurrence in different geographic regions. Annual precipitation (BIO12, dark blue) emerged as the primary limiting factor across extensive areas, including sub-Saharan Africa, Central Asia, interior Australia, and arid portions of the Americas. Minimum temperature of the coldest month (BIO6, light green) constituted the principal constraint across temperate and subtropical regions at higher latitudes, including southern Australia, temperate South America, and transitional zones in Asia and Africa. Precipitation of the wettest month (BIO13, medium blue) served as the dominant limiting factor in seasonally dry tropical and semi-arid regions, particularly in the African Sahel, parts of the Deccan Plateau, and northern Australia. Mean diurnal temperature range (BIO2, tan) and annual mean temperature (BIO1, orange) played more localized roles, primarily constraining distribution in highland tropical regions and latitudinal extremes, respectively.

Quantitative assessment demonstrated that precipitation-related variables collectively dominated as range-limiting factors, with BIO12 alone constraining 34.7% of analyzed areas, followed by BIO6 (28.3%) and BIO13 (18.9%) (Table 2). These patterns underscore the fundamental dependence of this aquatic fern on adequate moisture availability while highlighting the secondary but critical role of thermal constraints, particularly cold temperature extremes, in defining distributional boundaries. The dominance of water availability as a limiting factor emphasizes the species' vulnerability to projected changes in precipitation patterns under future climate scenarios, while temperature-limited regions may experience altered constraints as warming progresses.

Model performance and validation

The MaxEnt model demonstrated excellent predictive performance across multiple evaluation metrics. The Area Under the Receiver Operating Characteristic Curve (AUC) achieved a value of 0.91, substantially exceeding the threshold of 0.7 for acceptable performance and approaching the 0.9 benchmark for outstanding discrimination ability. The True Skill Statistic (TSS) yielded a value of 0.71, well above the 0.4 threshold for good performance and approaching the 0.75 benchmark for excellent performance. These metrics confirm that the model captured the environmental niche of *M. minuta* with high fidelity and possessed strong predictive capacity for projecting distributions under altered climate scenarios.

Environmental envelope analysis validated model reliability by examining the distribution of occurrence points within climate space defined by annual mean temperature (BIO1) and annual precipitation (BIO12) (Fig. 7). The bivariate plot revealed that 327 observations (90.6%) fell within the primary environmental envelope, while 235 observations (65.1%) clustered within core optimal conditions. Green points, representing presence records within well-sampled climate space, concentrated predominantly in mid-range temperature (18–26 °C) and precipitation (1000–2400 mm) gradients. Red points, indicating occurrences in marginal climate space, appeared scattered at distribution peripheries, particularly at temperature extremes and very high precipitation areas. This pattern demonstrates that model predictions were based primarily on interpolation within well-sampled environmental conditions rather than extrapolation beyond observed climate space. The environmental envelope test confirmed that future climate projections for all scenarios remained largely within observed climate space, with minimal extrapolation beyond current environmental conditions, thereby strengthening confidence in projected distributional shifts.

Variable contribution and response curves

Jackknife analysis of regularized training gain quantified the relative contribution of each environmental variable to model performance (Fig. 8). BIO1 (annual mean temperature) emerged as the most informative variable, with the isolated-variable model achieving a regularized training gain exceeding 1.2 and its exclusion causing the most dramatic performance decline. BIO6 (minimum temperature of coldest month) ranked second in importance, with its isolated model achieving a training gain approaching 0.9. BIO12 (annual precipitation) and BIO13 (precipitation of wettest month) showed intermediate importance, each contributing meaningfully when used alone (training gains of 0.5–0.6). BIO2 (mean diurnal range) demonstrated the lowest individual contribution, though its retention provided incremental improvements when combined with other variables.

Response curves illustrated the relationship between habitat suitability and each bioclimatic variable (Fig. 9). BIO1 exhibited a pronounced unimodal pattern, with suitability rising sharply between 5 and 15 °C, reaching maximum probability (0.65–0.70) at 20–25 °C, and declining above 30 °C, reflecting adaptation to warm tropical conditions. BIO2 showed a strongly negative relationship, with highest suitability at low diurnal ranges (2–4 °C) and monotonic decline as daily temperature variation increased, suggesting preference for thermally stable environments. BIO6 revealed relatively stable moderate probability across minimum temperatures from − 50 °C to 0 °C, followed by a sharp increase to maximum probability (0.70–0.75) between 0 and 15 °C, then declining above 20 °C. BIO12 exhibited a negative exponential response, likely reflecting marginal effects when other variables were held constant. BIO13 displayed a positive relationship, with probability increasing from 0.20 below 0 mm to maximum values (0.90–0.95) above 1200 mm, aligning with the species' dependence on seasonal water availability. Narrow confidence bands across response curves indicated robust and consistent relationships across model iterations.

Discussion

The MaxEnt species distribution model developed in this study demonstrated robust predictive performance, with AUC and TSS values of 0.91 and 0.71, respectively, indicating excellent discrimination ability and model accuracy. These performance metrics substantially exceed thresholds typically considered acceptable for ecological niche modeling applications and align with values reported for well-performing models across diverse plant taxa[45,60]. The high AUC value is consistent with previous MaxEnt applications for aquatic and semi-aquatic plant species, where model performance often benefits from the strong environmental filtering imposed by moisture requirements[16,61]. However, it is important to acknowledge that AUC values can be inflated when species exhibit highly restricted distributions or strong environmental preferences, potentially overestimating true predictive accuracy[54,62]. The complementary TSS metric, which accounts for both omission and commission errors while remaining independent of prevalence, provided a more conservative but equally positive assessment of model quality[55,56].

Bioclimatic Variable	Description	Area Constrained (%)	Rank	Primary Geographic Regions
BIO12	Annual Precipitation	34.7	1	Sub-Saharan Africa, Central Asia, Interior Australia, Arid Americas
BIO6	Min Temperature of Coldest Month	28.3	2	Temperate zones, Subtropical margins, Highland transitions
BIO13	Precipitation of Wettest Month	18.9	3	Seasonally dry tropics, Monsoon margins, Semi-arid regions
BIO2	Mean Diurnal Range	9.4	4	Highland tropics, Montane zones, Continental interiors
BIO1	Annual Mean Temperature	6.2	5	High latitudes, High elevations, Polar margins

Table 2. Relative importance of bioclimatic variables as limiting factors for *Marsilea minuta* distribution. Note: Percentages represent proportion of global land surface where each variable serves as the primary limiting factor for habitat suitability.

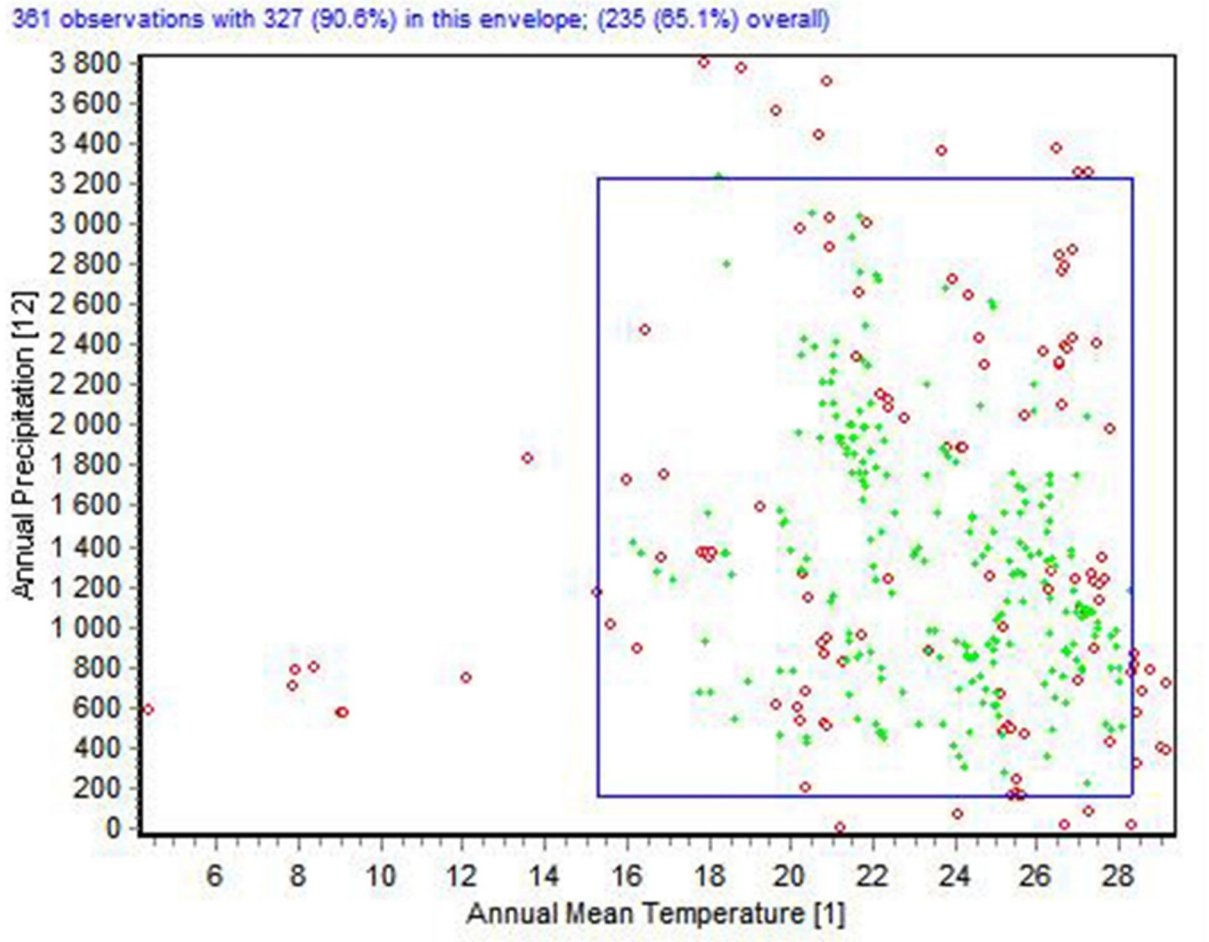

Fig. 7. Environmental envelope test displaying the distribution of *Marsilea minuta* occurrence records within climate space defined by annual mean temperature (BIO1, x-axis) and annual precipitation (BIO12, y-axis). Green points represent presence records falling within well-sampled regions of climate space, while red points indicate occurrences in marginal or extrapolated climate conditions. The rectangular boundary delineates the primary environmental envelope, with 327 observations (90.6%) falling within this space and 235 observations (65.1%) clustering within core optimal conditions at 18–26 °C and 1000–2400 mm precipitation, demonstrating that model predictions are based primarily on interpolation within observed climate space rather than extrapolation beyond known tolerance ranges.

The envelope test results indicating that future climate projections remained largely within current climate space suggest that predicted distributional changes represent shifts within the species' realized niche, as estimated from occurrence data (it should be noted that presence-only SDMs such as MaxEnt estimate the realized, not fundamental, niche, and therefore projections are bounded by observed species-environment relationships rather than the full physiological tolerance range) rather than exposure to entirely novel climate combinations, though this does not preclude the possibility of local extirpation due to habitat fragmentation or biotic interactions[63,64].

Variable contribution analysis identified annual mean temperature (BIO1) as the primary environmental determinant of *M. minuta* distribution, followed by minimum temperature of the coldest month (BIO6) and precipitation variables (BIO12 and BIO13). The dominance of temperature-related variables in defining habitat suitability reflects fundamental physiological constraints on plant metabolic processes, growth rates, and survival that are directly mediated by thermal conditions[65,66]. The unimodal response curve for BIO1, with optimal suitability between 20 and 25 °C and sharp declines at thermal extremes, is consistent with the tropical and subtropical distribution of Marsileaceae species and their evolutionary origins in warm, seasonally wet environments[5,6]. This thermal optimum aligns closely with temperature preferences documented for other aquatic macrophytes in tropical wetland systems, where temperatures exceeding 30 °C can impose metabolic stress and reduce photosynthetic efficiency, while temperatures below 15 °C may limit growth and reproductive output[67,68]. Comparison with other aquatic fern taxa provides useful phylogenetic context: studies on the floating ferns Azolla filiculoides and Salvinia molesta document similar thermal sensitivity, with optimal growth temperatures

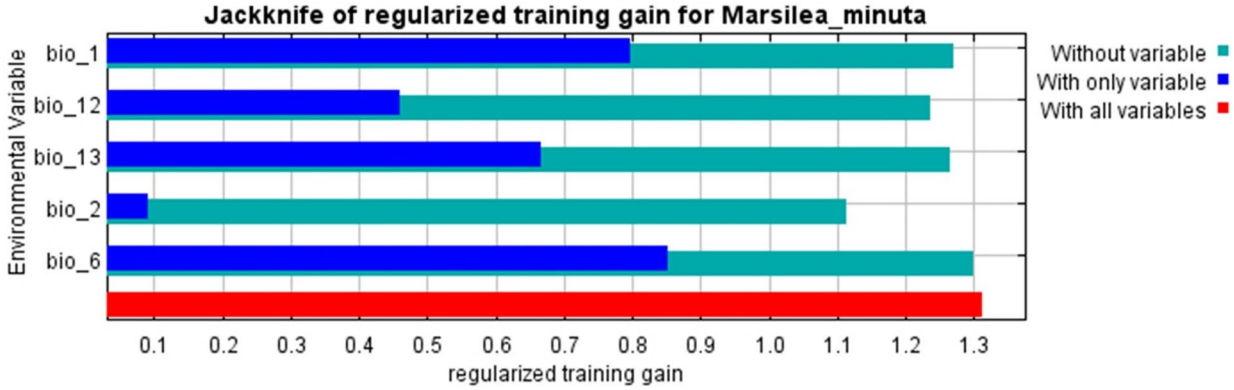

Fig. 8. Jackknife analysis of regularized training gain quantifying the relative contribution of each bioclimatic variable to MaxEnt model performance for *Marsilea minuta*. Light blue bars show model performance excluding each variable, dark blue bars represent performance with only that single variable, and the red line indicates performance with all variables included. BIO1 (annual mean temperature) provides the highest individual contribution with a training gain exceeding 1.2 when used alone, followed by BIO6 (minimum temperature of coldest month) with approximately 0.9, while BIO12, BIO13, and BIO2 demonstrate progressively lower individual contributions, though all variables contribute incrementally to overall model performance when combined.

between 20 and 28 °C and sharp declines at cold extremes[69,70]; Hill, 1998). However, Azolla and Salvinia show notably broader moisture tolerances and greater colonization capacity than *M. minuta*, suggesting that the strong precipitation constraints identified here may reflect lineage-specific traits of benthic Marsileaceae rather than a general functional response shared across aquatic fern taxa. This distinction underscores the importance of species-level SDM analyses for wetland conservation planning, as thermal and moisture thresholds cannot be reliably extrapolated across phylogenetically diverse aquatic ferns.

The strong contribution of BIO6 to model performance underscores the importance of cold temperature extremes in limiting poleward range expansion and defining distribution boundaries at higher latitudes and elevations. Minimum temperatures of the coldest month represent critical filters for species with limited frost tolerance, as even brief exposure to freezing conditions can cause tissue damage and mortality in tropical and subtropical plant species[71,72]. The response curve pattern, showing optimal suitability where minimum temperatures remain above 0 °C but below 15 °C, suggests that *M. minuta* requires frost-free conditions but benefits from some degree of seasonal temperature variation, possibly related to dormancy requirements or phenological cues for reproduction[73]. This thermal constraint has profound implications for climate change vulnerability, as warming winters may facilitate poleward range expansion into currently unsuitable temperate regions, though dispersal limitation and biotic resistance from established communities may prevent colonization of newly suitable areas[74,75].

Precipitation variables, particularly precipitation of the wettest month (BIO13), emerged as critical determinants of habitat suitability, reflecting the fundamental dependence of aquatic ferns on adequate water availability for completion of their life cycle. The positive relationship between BIO13 and occurrence probability aligns with the species' ecology as an obligate wetland inhabitant requiring seasonal or permanent water availability for spore germination, gametophyte development, and sporophyte establishment[76,77]. Peak wet-season precipitation represents a more reliable predictor of wetland habitat persistence than annual precipitation totals, as temporal concentration of rainfall determines whether ephemeral water bodies persist long enough to support aquatic plant populations[78,79]. The limiting factor analysis, which identified BIO12 as the primary constraint across 34.7% of analyzed areas, emphasizes that moisture availability constitutes the dominant range-limiting factor across vast regions where thermal conditions might otherwise be suitable, particularly in semi-arid and seasonally dry tropical zones[3,80].

Future distribution projections revealed substantial and spatially heterogeneous impacts of climate change on *M. minuta* habitat suitability, with net range contractions projected across all scenarios and time periods. The magnitude of predicted habitat loss increased progressively from near-term (2050) to mid-century (2070) projections and was consistently greater under high-emission (RCP 8.5) compared to low-emission (RCP 2.6) pathways, demonstrating the potential efficacy of climate mitigation in reducing biodiversity impacts[81,82]. Net range contractions ranging from 7.3% under the most optimistic scenario to 17.2% under the most severe scenario fall within the range of impacts predicted for tropical and subtropical plant species in recent meta-analyses, which estimate median range losses of 10–30% by mid-century under business-as-usual emission trajectories[1,10]. However, these projected losses may underestimate true extinction risk, as species distribution models typically do not account for additional stressors such as habitat fragmentation, land use change, altered disturbance regimes, and biotic interactions that can amplify climate change impacts[83,84].

The spatial pattern of projected changes, characterized by habitat losses concentrated at range margins and gains restricted to isolated pockets at higher latitudes, reflects the asymmetric nature of climate-driven range shifts for tropical species. While poleward expansion might theoretically compensate for tropical contractions,

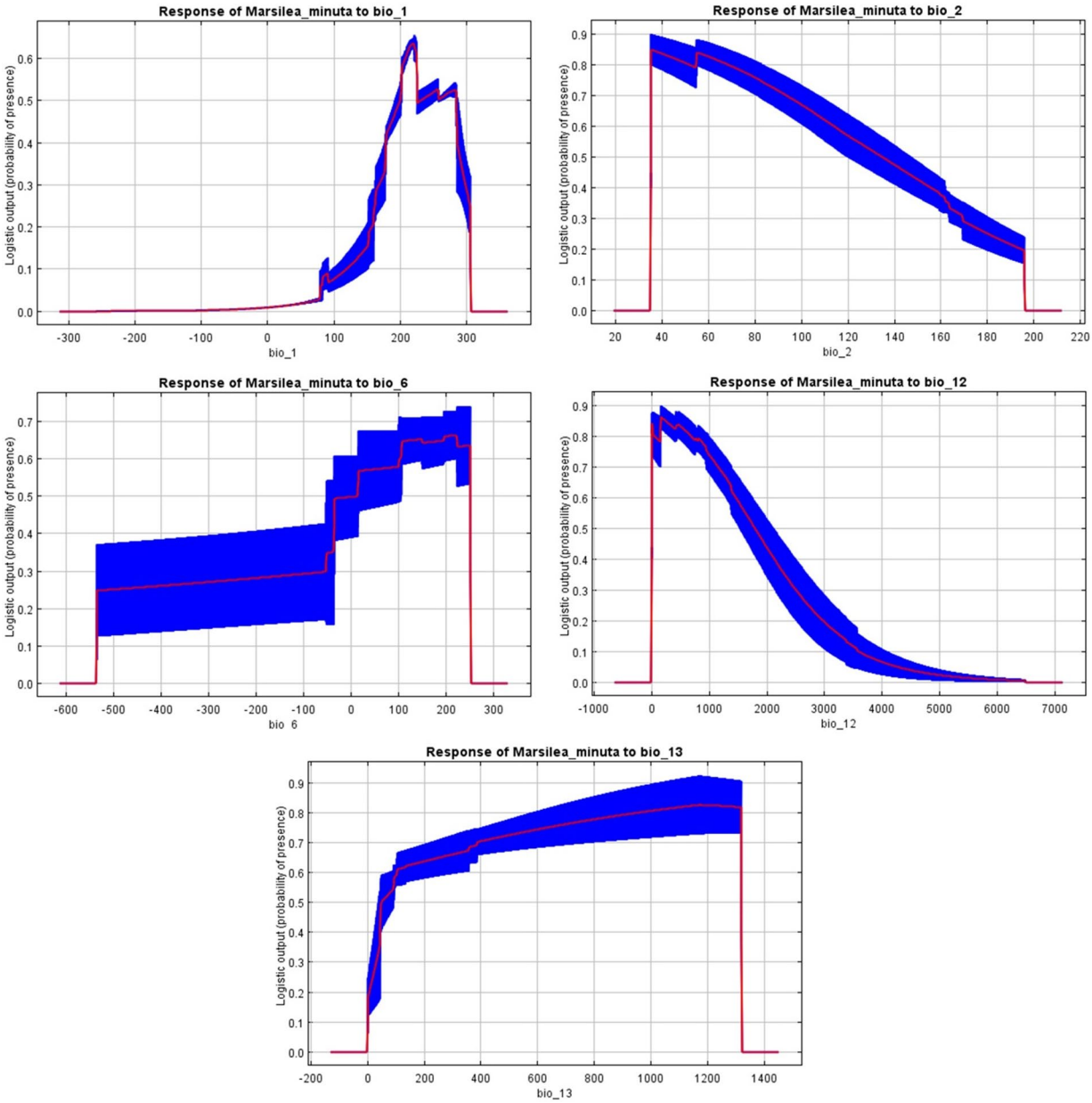

Fig. 9. Response curves illustrating the relationship between habitat suitability probability (y-axis) and each bioclimatic variable (x-axis) for *Marsilea minuta*, generated by MaxEnt while holding other variables at their mean values. The blue shaded area represents the range of predictions across 10 bootstrap replicate runs, with the red line showing the mean response. BIO1 exhibits a unimodal response with optimal suitability at 20–25 °C, BIO2 shows a negative relationship favoring low diurnal temperature ranges, BIO6 displays maximum probability between 0–15 °C minimum temperatures, BIO12 demonstrates a negative exponential pattern reflecting marginal effects, and BIO13 exhibits a positive relationship with highest suitability above 1200 mm wet-season precipitation.

realized range shifts are often limited by dispersal constraints, habitat availability, and priority effects from established species in newly suitable areas[85,86]. For aquatic plants dependent on ephemeral wetland habitats, dispersal between isolated suitable areas represents a particularly acute challenge, as wetland fragmentation has intensified globally due to agricultural conversion and drainage[87,88]. The capacity of *M. minuta* to colonize newly suitable areas will depend critically on dispersal vectors, including waterbirds and human-mediated transport, which may facilitate long-distance dispersal but operate at rates potentially insufficient to track rapidly shifting climate envelopes[11,89].

Regions identified as stable suitable habitat across multiple scenarios, particularly in South Asia and equatorial Africa, represent potential climate refugia that should be prioritized for conservation action. Climate refugia—areas where suitable environmental conditions persist despite regional climate change—can serve

as sources for population recovery and recolonization following climate-driven extirpations in surrounding areas[90,91]. The concentration of stable habitat in monsoon-influenced tropical lowlands suggests that regions maintaining reliable seasonal precipitation patterns may provide the most resilient habitat for moisture-dependent aquatic species under future climates. However, even within identified refugia, local threats such as agricultural intensification, wetland drainage, and invasive species may undermine conservation value and prevent populations from persisting despite climatically suitable conditions[92,93].

While this study provides valuable insights into potential climate change impacts on *M. minuta*, several sources of uncertainty warrant consideration when interpreting results. First, reliance on a single general circulation model (BCC-CSM1.1) limits our ability to capture the full range of uncertainty in future climate projections. Ensemble modeling approaches incorporating multiple GCMs have been shown to provide more robust predictions by accounting for inter-model variability in regional climate projections, though computational constraints often necessitate model selection trade-offs[18,94]. Second, the use of presence-only data and pseudo-absence points introduces potential biases related to sampling effort, spatial autocorrelation, and incomplete detection of suitable but unoccupied habitat[50,95]. While spatial filtering reduced sampling bias and model evaluation metrics indicated strong performance, true absence data would strengthen model calibration and provide more rigorous assessment of commission errors[51,96]. Fifth, it is important to emphasize that the correlative SDM framework employed here cannot establish mechanistic causation between climate variables and species occurrence, and projections should be interpreted as potential scenarios rather than definitive predictions[13]. The results indicate tendencies and relative vulnerabilities under modeled scenarios, but real-world outcomes will depend critically on local-scale processes, land-use dynamics, and ecological interactions not captured in bioclimatic models. Accordingly, conservation decisions should treat these projections as one line of evidence among many rather than as precise forecasts. Sixth, the Pearson correlation-based variable selection, even when supplemented by VIF analysis, may not fully eliminate complex non-linear collinear relationships among climatic predictors; future studies should consider regularized regression or algorithmic variable selection approaches to further improve predictor independence[97]. Collectively, these limitations suggest that the quantitative projections reported here (e.g., specific percentage range losses) should be interpreted with appropriate caution and as order-of-magnitude estimates rather than precise figures[98[,99].

Third, species distribution models inherently assume niche conservatism—that species-environment relationships remain constant through time—an assumption that may be violated if populations adapt to novel climatic conditions or if biotic interactions alter realized niches under future climates[100,101]. Adaptive capacity through phenotypic plasticity or evolutionary change could potentially allow *M. minuta* to tolerate environmental conditions beyond those observed in current populations, though rates of contemporary evolution are unlikely to match projected rates of climate change for most species[102,103]. Fourth, projections do not incorporate potential changes in other critical environmental factors such as atmospheric CO_2 concentration, nutrient availability, disturbance regimes, or biotic interactions with competitors, herbivores, and pathogens, all of which may interact with climate to influence species distributions[1,104]. Elevated CO_2 concentrations, for instance, may enhance aquatic plant productivity in some systems while altering competitive hierarchies in ways that could either benefit or disadvantage *M. minuta* relative to co-occurring species[105,106].

The projected climate-driven range contractions and habitat losses for *M. minuta* underscore the urgent need for proactive conservation strategies that account for both current threats and anticipated future changes. Protected area networks should be evaluated and potentially expanded to encompass identified climate refugia, particularly in South and Southeast Asia where stable suitable habitat is predicted to persist across multiple scenarios[107,108]. However, static protected area boundaries may prove insufficient for conserving species experiencing range shifts, necessitating more dynamic approaches that facilitate species tracking of shifting climate envelopes[109]. Climate-adaptive management strategies might include restoration and creation of wetland stepping-stones to enhance connectivity between isolated habitat patches, thereby facilitating dispersal and colonization of newly suitable areas[110,111].

Ex situ conservation measures, including germplasm banking and cultivation in botanical gardens, represent important complementary strategies for safeguarding genetic diversity and providing insurance against catastrophic population losses[112,113]. For aquatic ferns, spore banking offers a particularly effective ex situ approach, as spores can remain viable for extended periods under controlled storage conditions and can be used for population reinforcement or reintroduction if in situ populations decline[114]. Assisted colonization—the intentional translocation of species to areas currently beyond their range but predicted to become suitable under future climates—remains controversial but may warrant consideration for species facing severe range contractions and limited natural dispersal capacity, provided that rigorous risk assessments are conducted to prevent unintended ecological consequences[115,116].

Integration of climate change considerations into broader wetland conservation and restoration programs represents perhaps the most critical management priority. Maintaining and restoring the hydrological integrity of wetland systems, reducing nutrient pollution, controlling invasive species, and minimizing direct human disturbance will enhance the resilience of wetland ecosystems to climate change and improve the prospects for persistence of specialist species like *M. minuta*[117,118]. Land use planning that protects wetland networks and maintains connectivity between aquatic habitats will be essential for allowing species to shift their ranges in response to climate change while maintaining viable population sizes[119]. Ultimately, addressing the root cause of climate change through aggressive emissions reductions remains the most fundamental conservation action, as even the most sophisticated adaptation strategies will prove insufficient under scenarios of severe and accelerating climate disruption[9,120].

Data availability

All data are available through the manuscript and supplementary materials. Occurrence data are accessible through GBIF (GBIF.org, 2023). Climate data are available from WorldClim (worldclim.org).

Received: 1 February 2026; Accepted: 9 April 2026
Published online: 24 April 2026

References

1. Bellard, C., Bertelsmeier, C., Leadley, P., Thuiller, W. & Courchamp, F. Impacts of climate change on the future of biodiversity. *Ecol. Lett.* **15** (4), 365–377 (2012).
2. IPCC. *Climate Change 2021: The Physical Science Basis. Contribution of Working Group I to the Sixth Assessment Report of the Intergovernmental Panel on Climate Change* (Cambridge University Press, 2021).
3. Chambers, P. A., Lacoul, P., Murphy, K. J. & Thomaz, S. M. Global diversity of aquatic macrophytes in freshwater. *Hydrobiologia* **595** (1), 9–26 (2008).
4. Riis, T. et al. Ecosystem service delivery in urban river systems: A comparison of three rivers in different climatic zones. *Water* **12**(1), 179 (2020).
5. Johnson, D. M. Systematics of the New World species of *Marsilea* (Marsileaceae). *Syst. Bot. Monogr.* **11**, 1–87 (1986).
6. Launert, E. A monographic survey of the genus *Marsilea* Linnaeus. *Senckenb. Biol.* **49**, 273–315 (1968).
7. Joshi, S. V. & Janarthanam, M. K. The diversity of life-form type, habitat preference and phenology of the endemics in the Goa region of the Western Ghats, India. *J. Biogeogr.* **31**(8), 1227–1237 (2004).
8. Sharma, B. D. & Singh, N. P. *Flora of Nagaland: dicotyledons* (Botanical Survey of India, 2014).
9. Thomas, C. D. et al. Extinction risk from climate change. *Nature* **427** (6970), 145–148 (2004).
10. Urban, M. C. Accelerating extinction risk from climate change. *Science* **348** (6234), 571–573 (2015).
11. Hof, C., Levinsky, I., Araújo, M. B. & Rahbek, C. Rethinking species' ability to cope with rapid climate change. *Glob. Change Biol.* **17**(9), 2987–2990 (2011).
12. Elith, J. & Leathwick, J. R. Species distribution models: Ecological explanation and prediction across space and time. *Annu. Rev. Ecol. Evol. Syst.* **40**, 677–697 (2009).
13. Guisan, A. & Thuiller, W. Predicting species distribution: Offering more than simple habitat models. *Ecol. Lett.* **8**(9), 993–1009 (2005).
14. Elith, J. et al. A statistical explanation of MaxEnt for ecologists. *Diversity Distrib.* **17**(1), 43–57 (2011).
15. Phillips, S. J., Anderson, R. P. & Schapire, R. E. Maximum entropy modeling of species geographic distributions. *Ecol. Modell.* **190**(3–4), 231–259 (2006).
16. Fois, M., Cuena-Lombraña, A., Fenu, G. & Bacchetta, G. Using species distribution models at local scale to guide the search of poorly known species: Review, methodological issues and future directions. *Ecol. Modell.* **385**, 124–132 (2018).
17. Kumar, S. & Stohlgren, T. J. Maxent modeling for predicting suitable habitat for threatened and endangered tree *Canacomyrica monticola* in New Caledonia. *J. Ecol. Nat. Environ.* **1**(4), 94–98 (2009).
18. Araújo, M. B. & New, M. Ensemble forecasting of species distributions. *Trends Ecol. Evol.* **22**(1), 42–47 (2007).
19. Hannah, L. et al. Regional and local connectivity patterns of the critically endangered coastal heathland species *Erica cinerea* in future climate scenarios. *Glob. Ecol. Conserv.* **22**, e00944 (2020).
20. Broennimann, O. et al. Do geographic distribution, niche property and life form explain plants' vulnerability to global change?. *Glob. Change Biol.* **12**(6), 1079–1093 (2006).
21. Fitzpatrick, M. C. & Hargrove, W. W. The projection of species distribution models and the problem of non-analog climate. *Biodivers. Conserv.* **18** (8), 2255–2261 (2009).
22. Liu, C., Berry, P. M., Dawson, T. P. & Pearson, R. G. Selecting thresholds of occurrence in the prediction of species distributions. *Ecography* **28** (3), 385–393 (2005).
23. Riis, T. et al. Growth and morphology in relation to temperature and light availability during the establishment of three invasive aquatic plant species. *Aquat. Bot.* **102**, 56–64 (2012).
24. Edwards, J. L. Research and societal benefits of the Global Biodiversity Information Facility. *BioScience* **54**(6), 485–486 (2004).
25. Yesson, C. et al. How global is the global biodiversity information facility?. *PLoS One* **2**(11), p.e1124 (2007).
26. Hijmans, R. J., Cameron, S. E., Parra, J. L., Jones, P. G. & Jarvis, A. Very high resolution interpolated climate surfaces for global land areas. *Int. J. Climatol.* **25** (15), 1965–1978 (2005).
27. Kramer-Schadt, S. et al. The importance of correcting for sampling bias in MaxEnt species distribution models. *Divers. Distrib.* **19**(11), 1366–1379 (2013).
28. Zizka, A. et al. CoordinateCleaner: Standardized cleaning of occurrence records from biological collection databases. *Methods Ecol. Evol.* **10**(5), 744–751 (2019).
29. Aiello-Lammens, M. E., Boria, R. A., Radosavljevic, A., Vilela, B. & Anderson, R. P. spThin: An R package for spatial thinning of species occurrence records for use in ecological niche models. *Ecography* **38**(5), 541–545 (2015).
30. Boria, R. A., Olson, L. E., Goodman, S. M. & Anderson, R. P. Spatial filtering to reduce sampling bias can improve the performance of ecological niche models. *Ecol. Modell.* **275**, 73–77 (2014).
31. Fick, S. E. & Hijmans, R. J. WorldClim 2: New 1-km spatial resolution climate surfaces for global land areas. *Int. J. Climatol.* **37**(12), 4302–4315 (2017).
32. O'Donnell, M. S. & Ignizio, D. A. Bioclimatic predictors for supporting ecological applications in the conterminous United States. U.S. Geological Survey Data Series, 691, pp.1–10. (2012).
33. Escobar, L. E., Lira-Noriega, A., Medina-Vogel, G. & Peterson, A. T. Potential for spread of the white-nose fungus (*Pseudogymnoascus destructans*) in the Americas: Use of Maxent and NicheA to assure strict model transference. *Geospatial Health* **9**(1), 221–229 (2014).
34. Kriticos, D. J., Jarošik, V. & Ota, N. Extending the suite of Bioclim variables: A proposed registry system and case study using principal components analysis. *Methods Ecol. Evol.* **5**(9), 956–960 (2014).
35. Hijmans, R. J., Guarino, L., Cruz, M. & Rojas, E. Computer tools for spatial analysis of plant genetic resources data: 1. DIVA-GIS. *Plant Genet. Resour. Newsl.* **127**, 15–19 (2012).
36. Dormann, C. F. et al. Collinearity: A review of methods to deal with it and a simulation study evaluating their performance. *Ecography* **36**(1), 27–46 (2013).
37. Feng, X., Park, D. S., Liang, Y., Pandey, R. & Papeş, M. Collinearity in ecological niche modeling: Confusions and challenges. *Ecol. Evol.* **9**(18), 10365–10376 (2019).
38. O'Brien, R. M. A caution regarding rules of thumb for variance inflation factors. *Qual. Quant.* **41**(5), 673–690 (2007).
39. Radosavljevic, A. & Anderson, R. P. Making better Maxent models of species distributions: Complexity, overfitting and evaluation. *J. Biogeogr.* **41**(4), 629–643 (2014).
40. Wu, T. et al. An overview of BCC climate system model development and application for climate change studies. *Acta Meteorol. Sin.* **28**(1), 34–56 (2014).

41. Moss, R. H. et al. The next generation of scenarios for climate change research and assessment. *Nature* **463** (7282), 747–756 (2010).
42. van Vuuren, D. P. et al. The representative concentration pathways: An overview. *Clim. Change* **109**(1), 5–31 (2011).
43. Araújo, M. B., Alagador, D., Cabeza, M., Nogués-Bravo, D. & Thuiller, W. Climate change threatens European conservation areas. *Ecol. Lett.* **14**(5), 484–492 (2011).
44. Phillips, S. J. & Dudík, M. Modeling of species distributions with Maxent: New extensions and a comprehensive evaluation. *Ecography* **31**(2), 161–175 (2008).
45. Elith, J. et al. Novel methods improve prediction of species' distributions from occurrence data. *Ecography* **29**(2), 129–151 (2006).
46. Hernandez, P. A., Graham, C. H., Master, L. L. & Albert, D. L. The effect of sample size and species characteristics on performance of different species distribution modeling methods. *Ecography* **29** (5), 773–785 (2006).
47. Roberts, D. R. et al. Cross-validation strategies for data with temporal, spatial, hierarchical, or phylogenetic structure. *Ecography* **40**(8), 913–929 (2017).
48. Valavi, R., Elith, J., Lahoz-Monfort, J. J. & Guillera-Arroita, G. blockCV: An R package for generating spatially or environmentally separated folds for k-fold cross-validation of species distribution models. *Methods Ecol. Evol.* **10**(2), 225–232 (2019).
49. Barve, N. et al. The crucial role of the accessible area in ecological niche modeling and species distribution modeling. *Ecol. Modell.* **222**(11), 1810–1819 (2011).
50. Phillips, S. J. et al. Sample selection bias and presence-only distribution models: Implications for background and pseudo-absence data. *Ecol. Appl.* **19**(1), 181–197 (2009).
51. Barbet-Massin, M., Jiguet, F., Albert, C. H. & Thuiller, W. Selecting pseudo-absences for species distribution models: How, where and how many?. *Methods Ecol. Evol.* **3**(2), 327–338 (2012).
52. Fielding, A. H. & Bell, J. F. A review of methods for the assessment of prediction errors in conservation presence/absence models. *Environ. Conserv.* **24**(1), 38–49 (1997).
53. Swets, J. A. Measuring the accuracy of diagnostic systems. *Science* **240** (4857), 1285–1293 (1988).
54. Lobo, J. M., Jiménez-Valverde, A. & Real, R. AUC: A misleading measure of the performance of predictive distribution models. *Glob. Ecol. Biogeogr.* **17**(2), 145–151 (2008).
55. Allouche, O., Tsoar, A. & Kadmon, R. Assessing the accuracy of species distribution models: Prevalence, kappa and the true skill statistic (TSS). *J. Biogeogr.* **33**(12), 1763–1774 (2006).
56. Liu, C., White, M. & Newell, G. Selecting thresholds for the prediction of species occurrence with presence-only data. *J. Biogeogr.* **40** (4), 778–789 (2013).
57. Anderson, R. P. et al. *Final report of the task group on GARP best practices* (University of Kansas Natural History Museum, 2016).
58. Hijmans, R. J. & Graham, C. H. The ability of climate envelope models to predict the effect of climate change on species distributions. *Glob. Change Biol.* **12**(12), 2272–2281 (2006).
59. Elith, J., Kearney, M. & Phillips, S. The art of modelling range-shifting species. *Methods Ecol. Evol.* **1** (4), 330–342 (2010).
60. Peterson, A. T. et al. *Ecological Niches and Geographic Distributions* (Princeton University Press, 2011).
61. Guisan, A., Thuiller, W. & Zimmermann, N. E. *Habitat Suitability and Distribution Models: With Applications in R* (Cambridge University Press, 2017).
62. Peterson, A. T., Papeş, M. & Soberón, J. Rethinking receiver operating characteristic analysis applications in ecological niche modeling. *Ecol. Modell.* **213**(1), 63–72 (2008).
63. Stralberg, D. et al. Re-shuffling of species with climate disruption: A no-analog future for California birds?. *PLoS One* **4**(9), e6825 (2009).
64. Williams, J. W. & Jackson, S. T. Novel climates, no-analog communities, and ecological surprises. *Front. Ecol. Environ.* **5**(9), 475–482 (2007).
65. Araújo, M. B. & Peterson, A. T. Uses and misuses of bioclimatic envelope modeling. *Ecology* **93** (7), 1527–1539 (2012).
66. Woodward, F. I. *Climate and Plant Distribution* (Cambridge University Press, 1987).
67. Barko, J. W. & Smart, R. M. Comparative influences of light and temperature on the growth and metabolism of selected submersed freshwater macrophytes. *Ecol. Monogr.* **51**(2), 219–235 (1981).
68. Madsen, T. V. & Brix, H. Growth, photosynthesis and acclimation by two submerged macrophytes in relation to temperature. *Oecologia* **110** (3), 320–327 (1997).
69. Janes, R. Growth and survival of *Azolla filiculoides* in Britain. *Aquat. Bot.* **60**(4), 359–367 (1998).
70. Julien, M. H., Center, T. D. & Tipping, P. W. Floating fern (Salvinia). In: (eds Van Driesche, R. et al.) Biological Control of Invasive Plants in the Eastern United States. USDA Forest Service, 17–32. (2002).
71. Larcher, W. *Physiological Plant Ecology: Ecophysiology and Stress Physiology of Functional Groups* 4th edition. (Springer, 2003).
72. Sakai, A. & Larcher, W. *Frost Survival of Plants: Responses and Adaptation to Freezing Stress* (Springer-Verlag, 1987).
73. Baskin, C. C. & Baskin, J. M. *Seeds: Ecology, Biogeography, and Evolution of Dormancy and Germination* 2nd edition. (Academic Press, 2014).
74. Lenoir, J., Gégout, J. C., Marquet, P. A., De Ruffray, P. & Brisse, H. A significant upward shift in plant species optimum elevation during the 20th century. *Science* **320** (5884), 1768–1771 (2008).
75. Walther, G. R. et al. Ecological responses to recent climate change. *Nature* **416** (6879), 389–395 (2002).
76. Hickok, L. G. Cytological relationships between three diploid species of the fern genus *Ceratopteris*. *Can. J. Bot.* **55**(13), 1660–1667 (1977).
77. Schneller, J. J. & Kramer, K. U. Sexual reproduction and population biology. In: (ed Raghavan, V.) Biology and Systematics of Ferns. American Fern Society, 169–188. (1986).
78. Mitsch, W. J. & Gosselink, J. G. *Wetlands* 5th edition. (John Wiley & Sons, 2015).
79. Reid, A. J. et al. Emerging threats and persistent conservation challenges for freshwater biodiversity. *Biol. Rev.* **94**(3), 849–873 (2019).
80. Murphy, K. J. et al. Aquatic plant communities and predictors of diversity in a sub-tropical river floodplain: The upper Rio Paraná, Brazil. *Aquat. Bot.* **77**(3), 257–276 (2003).
81. Pacifici, M. et al. Assessing species vulnerability to climate change. *Nat. Clim. Chang.* **5**(3), 215–224 (2015).
82. Warren, R. et al. Quantifying the benefit of early climate change mitigation in avoiding biodiversity loss. *Nat. Clim. Change* **3**(7), 678–682 (2013).
83. Brook, B. W., Sodhi, N. S. & Bradshaw, C. J. Synergies among extinction drivers under global change. *Trends Ecol. Evol.* **23**(8), 453–460 (2008).
84. Mantyka-Pringle, C. S., Martin, T. G. & Rhodes, J. R. Interactions between climate and habitat loss effects on biodiversity: A systematic review and meta-analysis. *Glob. Change Biol.* **18**(4), 1239–1252 (2012).
85. Alexander, J. M. et al. Lags in the response of mountain plant communities to climate change. *Glob. Change Biol.* **22**(2), 563–579 (2016).
86. Angert, A. L. et al. Do species' traits predict recent shifts at expanding range edges?. *Ecol. Lett.* **14**(7), 677–689 (2011).
87. Davidson, N. C. How much wetland has the world lost? Long-term and recent trends in global wetland area. *Mar. Freshw. Res.* **65**(10), 934–941 (2014).
88. Hu, S., Niu, Z., Chen, Y., Li, L. & Zhang, H. Global wetlands: Potential distribution, wetland loss, and status. *Sci. Total Environ.* **586**, 319–327 (2017).

89. Figuerola, J. & Green, A. J. Dispersal of aquatic organisms by waterbirds: A review of past research and priorities for future studies. *Freshw. Biol.* **47**(3), 483–494 (2002).
90. Keppel, G. et al. Refugia: Identifying and understanding safe havens for biodiversity under climate change. *Glob. Ecol. Biogeogr.* **21**(4), 393–404 (2012).
91. Morelli, T. L. et al. Managing climate change refugia for climate adaptation. *PLoS One*. **11** (8), e0159909 (2016).
92. Finlayson, C. M., Davidson, N. C., Spiers, A. G. & Stevenson, N. J. Global wetland inventory–current status and future priorities. *Mar. Freshw. Res.* **56**(5), 617–627 (2005).
93. Sala, O. E. et al. Global biodiversity scenarios for the year 2100. *Science* **287** (5459), 1770–1774 (2000).
94. Buisson, L., Thuiller, W., Casajus, N., Lek, S. & Grenouillet, G. Uncertainty in ensemble forecasting of species distribution. *Glob. Change Biol.* **16** (4), 1145–1157 (2010).
95. Fourcade, Y., Engler, J. O., Rödder, D. & Secondi, J. Mapping species distributions with MAXENT using a geographically biased sample of presence data: A performance assessment of methods for correcting sampling bias. *PLoS One* **9**(5), e97122 (2014).
96. Lobo, J. M., Jiménez-Valverde, A. & Hortal, J. The uncertain nature of absences and their importance in species distribution modelling. *Ecography* **33**(1), 103–114 (2010).
97. Naimi, B., Hamm, N. A., Groen, T. A., Skidmore, A. K. & Toxopeus, A. G. Where is positional uncertainty a problem for species distribution modelling?. *Ecography* **37**(2), 191–203 (2014).
98. SAS Institute Inc. *JMP Pro 16* (SAS Institute Inc., 2019).
99. Thuiller, W., Lavorel, S., Araújo, M. B., Sykes, M. T. & Prentice, I. C. Climate change threats to plant diversity in Europe. *Proc. Natl. Acad. Sci. U. S. A.* **102**(23), 8245–8250 (2005).
100. Hoffmann, A. A. & Sgrò, C. M. Climate change and evolutionary adaptation. *Nature* **470** (7335), 479–485 (2011).
101. Pearman, P. B., Guisan, A., Broennimann, O. & Randin, C. F. Niche dynamics in space and time. *Trends Ecol. Evol.* **23**(3), 149–158 (2008).
102. Hoffmann, A. A., Chown, S. L. & Clusella-Trullas, S. Upper thermal limits in terrestrial ectotherms: How constrained are they?. *Funct. Ecol.* **27**(4), 934–949 (2017).
103. Quintero, I. & Wiens, J. J. Rates of projected climate change dramatically exceed past rates of climatic niche evolution among vertebrate species. *Ecol. Lett.* **16** (8), 1095–1103 (2013).
104. Broennimann, O. et al. Evidence of climatic niche shift during biological invasion. *Ecol. Lett.* **10**(8), 701–709 (2007).
105. Grutters, B. M., Gross, E. M. & Bakker, E. S. Insect herbivory on native and exotic aquatic plants: Phosphorus and nitrogen drive insect growth and nutrient release. *Hydrobiologia* **778**(1), 209–220 (2017).
106. Hussner, A. et al. Management and control methods of invasive alien freshwater aquatic plants: A review. *Aquat. Bot.* **136**, 112–137 (2016).
107. Hannah, L. et al. Protected area needs in a changing climate. *Front. Ecol. Environ.* **5**(3), 131–138 (2007).
108. Kujala, H., Moilanen, A., Araújo, M. B. & Cabeza, M. Conservation planning with uncertain climate change projections. *PLoS One*. **8** (2), e53315 (2013).
109. Lawler, J. J., Ruesch, A. S., Olden, J. D. & McRae, B. H. Projected climate-driven faunal movement routes. *Ecol. Lett.* **16**(8), 1014–1022 (2015).
110. Hodgson, J. A., Thomas, C. D., Wintle, B. A. & Moilanen, A. Climate change, connectivity and conservation decision making: Back to basics. *J. Appl. Ecol.* **46**(5), 964–969 (2009).
111. Nuñez, T. A. et al. Connectivity planning to address climate change. *Conserv. Biol.* **27**(2), 407–416 (2013).
112. Liu, U. et al. Conserving orthodox seeds of globally threatened plants ex situ in the Millennium Seed Bank, Royal Botanic Gardens, Kew, UK: The status of seed collections. *Biodivers. Conserv.* **24**(4), 785–794 (2015).
113. Pence, V. C. Tissue cryopreservation for plant conservation: Potential and challenges. *Int. J. Plant Sci.* **175**(1), 40–45 (2014).
114. Pence, V. C. In vitro methods and the challenge of exceptional species for target 8 of the global strategy for plant conservation. *Ann. Mo. Bot. Gard.* **99**(2), 214–220 (2013).
115. Hewitt, N. et al. Taking stock of the assisted migration debate. *Biol. Conserv.* **144**(11), 2560–2572 (2011).
116. Schwartz, M. W. et al. Managed relocation: Integrating the scientific, regulatory, and ethical challenges. *BioScience* **62**(8), 732–743 (2012).
117. Erwin, K. L. Wetlands and global climate change: The role of wetland restoration in a changing world. *Wetl. Ecol. Manage.* **17**(1), 71–84 (2009).
118. Finlayson, C. M., Horwitz, P. & Weinstein, P. *Wetlands and Human Health* (Springer Science & Business Media, 2013).
119. Foden, W. B. et al. Identifying the world's most climate change vulnerable species: A systematic trait-based assessment of all birds, amphibians and corals. *PLoS One* **8**(6), e65427 (2013).
120. Scheffers, B. R. et al. The broad footprint of climate change from genes to biomes to people. *Science* **354** (6313), aaf7671 (2016).

Acknowledgements

The authors would like to extend their sincere appreciation to the Ongoing Research Funding Program (ORF-2026-686), King Saud University, Riyadh, Saudi Arabia.

Author contributions

S.K.: Conceptualization, Methodology, Investigation, Formal Analysis, Writing - Original Draft, Writing - Review & Editing, Validation, Data Curation, Supervision. A.G.: Methodology, Investigation, Writing - Original Draft. M.W..: Software, Validation, Investigation, Writing - Review & Editing. M.T.: Conceptualization, Methodology, Writing - Original Draft, Validation, Data curation, Supervision.

Funding

No funds were received for conducting this study.

Declarations

Competing interests

The authors declare no competing interests.

Additional information

Correspondence and requests for materials should be addressed to S.M.K.

Reprints and permissions information is available at www.nature.com/reprints.